Available online at www.sciencedirect.com

ScienceDirect

Genomics 89 (2007) 262–269

GENOMICS

www.elsevier.com/locate/ygeno

YY1 as a controlling factor for the *Peg3* and *Gnas* imprinted domains

Jeong Do Kim [a], Angela K. Hinz [b], Jung Ha Choo [a], Lisa Stubbs [b], Joomyeong Kim [a,*]

[a] *Department of Biological Sciences, Center for BioModular Multi-Scale Systems, Louisiana State University, Baton Rouge, LA 70803, USA*
[b] *Genome Biology Division, Lawrence Livermore National Laboratory, Livermore, CA 94551, USA*

Received 8 August 2006; accepted 25 September 2006
Available online 25 October 2006

Abstract

Imprinting control regions (ICRs) often harbor tandem arrays of transcription factor binding sites, as demonstrated by the identification of multiple YY1 binding sites within the ICRs of *Peg3, Nespas*, and *Xist/Tsix* domains. In the current study, we have sought to characterize possible roles for YY1 in transcriptional control and epigenetic modification of these imprinted domains. RNA interference-based knockdown experiments in Neuro2A cells resulted in overall transcriptional up-regulation of most of the imprinted genes within the *Peg3* domain and also, concomitantly, caused significant loss in the DNA methylation of the *Peg3* differentially methylated region. A similar overall and coordinated expression change was also observed for the imprinted genes of the *Gnas* domain: up-regulation of *Nespas* and down-regulation of *Nesp* and *Gnasxl*. YY1 knockdown also resulted in changes in the expression levels of *Xist* and *Snrpn*. These results support the idea that YY1 plays a major role, as a *trans* factor, in the control of these imprinted domains.
Published by Elsevier Inc.

Keywords: Genomic imprinting; ICRs; YY1

A small number of mammalian genes are subject to an unusual dosage control, called genomic imprinting, in which one of two alleles of the genes is repressed in a parental-origin-specific manner. The imprinted genes are clustered in specific regions of chromosomes, and each imprinted domain is typically controlled by small genomic regions, termed imprinting control regions (ICRs) [1–3]. These ICRs are usually located in CpG-rich regions near the promoters of imprinted genes and methylated differentially between the two parental alleles. These regions often show tandem repeat sequence structure [4,5] and the core sequences of these tandem repeats have been shown in several cases to correspond to transcription factor binding sites. Known transcription factors binding to repeat regions include CTCF for the ICR of the *H19/Igf2* imprinted domain and YY1 for the differentially methylated region (DMR) of the *Peg3, Nespas*, and *Xist/Tsix* imprinted domains [6–9]. In the *H19/Igf2* imprinted domain, CTCF functions as an enhancer-blocker for controlling allele-specific expression of *H19* and *Igf2* [10,11]. However, the in vivo functions of YY1 for the *Peg3* and other imprinted domains require further investigation.

The mammalian transcription factor YY1 is a ubiquitously expressed, multifunctional protein that can function as an activator, repressor, or initiator binding protein depending upon the sequence context of YY1 binding sites with respect to other regulator elements (reviewed in [12–14]). The protein has a DNA binding domain at the C-terminus and other modulating domains at the N-terminus displaying repression, activation, and protein–protein interaction activities. YY1 interacts with several key components of general Pol II transcription machineries, including TBP, TAFs, and TFIIB, as well as histone-modifying enzymes, including p300, HDACs, and PRMT1 (reviewed in [12–14]). YY1 is evolutionarily well conserved throughout all vertebrate lineages and at least two genes similar to vertebrate *YY1* are found in fly genomes. One of these YY1 homologues is involved in the Polycomb complex-mediated repression mechanism [15]. Recent studies also support a similar role for YY1 in this heritable silencing mechanism of vertebrates [16,17]. We have previously identified an unusual tandem array of multiple YY1 binding sites located within the *Peg3* DMR [8] and later confirmed the presence of similar clustered YY1 binding sites within the ICRs of *Xist, Tsix*, and *Nespas* [9]. The localization of these multiple YY1 binding sites within imprinting control regions is very

* Corresponding author. Fax: +1 225 578 2597.
E-mail address: jkim@lsu.edu (J. Kim).

0888-7543/$ - see front matter. Published by Elsevier Inc.
doi:10.1016/j.ygeno.2006.09.009

unusual and suggests a potential role for YY1 in mammalian genomic imprinting.

In the current study, we have lowered the YY1 protein levels through RNA interference techniques and subsequently analyzed the short- and long-term effects of this YY1 knockdown on the transcription and DNA methylation of the *Peg3* DMR and other YY1-associated genomic regions. Our results indicate that YY1 may function as a controlling factor for the *Peg3* and *Gnas* imprinted domains and also that YY1 may be involved in maintaining the proper methylation status of these differentially methylated, imprinting control regions.

Results

The short-term effects of YY1 knockdown on the transcription of the Peg3 domain

Of three siRNA constructs designed to knock down YY1, we found one construct that consistently lowered the YY1 protein level in transiently transfected cells of both Neuro2A (Fig. 1A) and NIH3T3 lines (data not shown). Western blot analyses indicated up to 90% reduction in the YY1 protein level in the cells transiently transfected with this YY1-siRNA construct, while control cells with no transfection (NT) and with transfection using another siRNA construct containing a scrambled sequence (Scr) showed no change in the YY1 protein level. Two independent Western blots using β-actin and p53 antibodies also confirmed the target-specific knockdown of YY1 by this siRNA construct.

We analyzed the short-term (transient) effects of the YY1 knockdown on the transcription of the endogenous loci that are known to be associated with YY1 binding sites [9]. For this series of tests, total RNA was first isolated from two different pools of cells that had each been transiently transfected with the Scr- or the YY1-siRNA construct and used to generate cDNA for real-time quantitative RT-PCR. In this qRT-PCR scheme, the relative abundance of a given mRNA between two types of cells was measured by the difference in the arbitrary C_t (threshold cycle) values. As shown in Fig. 1B, the set of 19 genes analyzed in this assay showed a broad range of averaged C_t values, indicating a wide range of expression levels among the individual genes in Neuro2A cells. The internal control genes that were used for the normalization of two different amounts of cDNA templates showed higher expression levels (β-*actin, GAPDH, 28S*). In contrast, the three genes that were included to monitor interferon response showed much lower expression levels (*Oas2, Mx1, IFMT1*), confirming no interferon response in our siRNA transfection experiments [18,19]. The imprinted genes in the *Peg3* domain (Fig. 2C; *Peg3, Usp29, Zim1, Zim2, Zim3, Zfp264*) also showed a

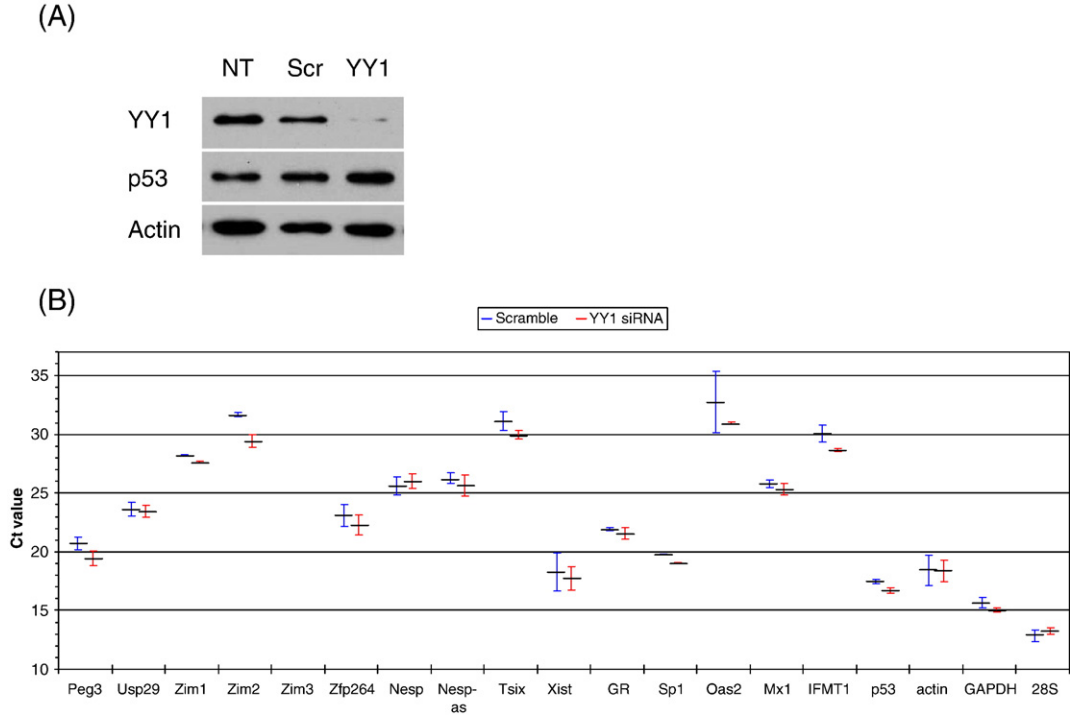

Fig. 1. Short-term effects of transient YY1 knockdown on transcription. (A) Target-specific YY1 knockdown by YY1 siRNA. The protein extracts prepared from Neuro2A cells were not transfected (NT) or were transfected with a scramble siRNA control (Scr) or YY1 siRNA construct (YY1) and analyzed with Western blotting using polyclonal antibodies against YY1, p53, and β-actin. Very low levels (~10%) of the YY1 protein were detected in the sample derived from YY1-siRNA-transfected cells. (B) Short-term effects of YY1 knockdown on the transcriptional levels of various genes. Reverse transcription and subsequent qRT-PCR were performed using two pools of total RNAs isolated from Scr-siRNA- and YY1-siRNA-transfected Neuro2A cells. The relative expression level of each gene, the name of which is shown on the *x* axis of the graph, was represented by an arbitrary threshold cycle (C_t) number shown on the *y* axis of the graph. The lower C_t values mean higher expression levels of the tested genes. The result set shown here is a summary of more than three independent trials, starting from transfection to qRT-PCR. The C_t value of each gene in a given trial was first normalized with ubiquitously expressing control genes (β-*actin, GAPDH*, and *28S*) and later averaged with the values from other trials. The C_t value with standard deviation (SD) on the left for each gene was derived from Scr-siRNA-transfected cells, while the right value is from YY1-siRNA-transfected cells.

wide range of expression levels in Neuro2A cells. *Peg3*, also known as *Pw1* [20], showed the highest expression level, whereas *Zim3* expression was not detectable at all. Comparison of C_t values of these genes revealed up-regulation of *Peg3, Zim1*, and *Zim2* in the YY1-siRNA-transfected cells. By contrast, the C_t value difference for *Usp29* and *Zfp264* may not be significant since two C_t values overlap within error ranges. We also tested the effects of YY1 knockdown on the expression levels of other YY1-associated genes, such as the genes in the *Gnas* and *Xist/Tsix* domains as well as other nonimprinted genes, including *Sp1* and *GR* (glucocorticoid receptor). Except for slight up-regulation in *Sp1*, most genes were not affected by transient YY1 knockdown. Overall, our transient knockdown experiments hinted at one possibility that lowering the YY1 protein level may have an immediate impact, specifically, up-regulation, on the transcription of several genes in the *Peg3* imprinted domain.

The long-term effects of YY1 knockdown on the transcription of imprinted domains

Using an RNAi strategy similar to that described above, we also analyzed the long-term effects of YY1 knockdown on the transcription of the genes located within the *Peg3*- and other YY1-associated imprinted domains. For this analysis, an inverted DNA sequence derived from mouse YY1 was incorporated into the 3′-UTR of the β-galactosidase gene in the pcDNA3.1/His/lacZ vector (Invitrogen). This scheme allowed us to monitor easily the expression of the YY1-targeting RNA portion by in situ β-galactosidase staining. This construct along with a control pcDNA3.1/His/lacZ vector without the YY1-targeting portion (EV; empty vector) was transfected individually into Neuro2A cells to derive stable cell lines using G418 selection. Of six stable single cell lines isolated, two cell lines (Nos. 6-2 and 6-4) showed the lowest levels of the YY1 protein (Fig. 2A) and thus were selected for our analyses. Total RNA was first isolated from four different types of cells: two control cells, NT and EV, and two YY1 knockdown cells, 6-2 and 6-4. These isolated RNAs were used to compare the expression levels of a given gene among the different cells using (1) RT-PCR with fixed numbers of cycles, 30 to 35 (Fig. 2B), and (2) quantitative RT-PCR (Figs. 2C and 2D).

In the *Peg3* imprinted domain, the expression of most of the resident genes except for *Zim3* was detectable in the Neuro2A-derived stable cells, and also the expression levels of *Peg3, Usp29*, and *Zim1* differed in two YY1 knockdown cells relative to the control cell lines. Another series of independent qRT-PCR analyses further confirmed that the expression levels of these three genes in the YY1 knockdown cell lines were higher than those of the control cell set, ranging from three- to fivefold (Fig. 2C). This increase in expression levels in *Peg3, Usp29*, and *Zim1* is consistent with the slight up-regulation of *Peg3, Zim1*, and *Zim2* that was observed from the transient YY1 knockdown experiments (Fig. 1B). It is interesting that, in both cases, more than one gene was affected similarly by YY1 knockdown.

In the *Gnas* domain, however, stable YY1 knockdown had opposite effects among the resident genes: whereas *Nespas* expression was increased (threefold), decreased expression of *Nesp* (three- to fourfold) and *Gnasxl* (fivefold) was observed in the YY1 knockdown cell lines (Figs. 2B and 2C). Given the frequent detection of coregulation between sense and antisense gene pairs in imprinted domains, the up- and down-regulation of *Nespas/Nesp* may represent two connected outcomes. By contrast, the expression levels of an alternative transcript, *Exon1A*, were relatively low with no obvious difference among the cells except for the slight increase observed in the 6-4 cell.

In contrast to genes in the *Peg3* and *Gnas* imprinted domains, the knockdown effects in stable cells were somewhat less obvious for other YY1-related genes, such as *Xist* and *Snrpn*, the latter of which is another YY1-involved imprinted gene identified independently by others [21]. Despite the fact that we detected no obvious difference by RT-PCR, qRT-PCR analyses revealed that *Xist* expression levels were slightly increased by 1.5- to 2-fold in the YY1 knockdown cells (Fig.

Fig. 2. Long-term effects of YY1 knockdown on transcription. (A) Stable transfectants with YY1 knockdown. To derive stable transfectants with YY1 knockdown, a commercial vector, pcDNA3.1/His/lacZ (Invitrogen) was modified by subcloning the YY1-targeting RNA portion into the 3′-UTR of the β-*Gal* gene in this vector. This vector along with another control vector lacking the YY1-targeting portion (empty vector, EV) was transfected into Neuro2A cells and selected with G418 (500 μg/ml). Six isolated single cell lines (Nos. 6-1 through 6-6) were analyzed with Western blotting using polyclonal antibodies against YY1 and β-actin. The density of individual bands on the developed films was first measured using the Gel Doc system (Bio-Rad), and later the normalized band densities relative to those of β-actin were calculated and used for determining the levels of YY1 knockdown. The lowest levels of YY1 were detected in two isolated cell lines, 6-2 and 6-4, compared to the YY1 levels of NT (no transfection) and EV. (B) Long-term effects on transcriptional levels of genes by YY1 knockdown. Long-term effects of YY1 knockdown were measured first by RT-PCR with fixed number of cycles ranging from 30 to 35. The expression levels of each gene were compared among four different cells: lane 1, no transfection; lane 2, transfection with the EV vector lacking the YY1-targeting region; lane 3, stable transfectant 6-2; lane 4, stable transfectant 6-4. All the tested genes were grouped together based on the chromosomal location (*Peg3* and *Gnas* domain), their association with YY1 (YY1 related genes), and also their purposes for our experiments (Control and Side effect). We also included the analyses of DNA methyltransferases (DNMTs) to test the YY1 knockdown effects on the DNA methylation of several loci as shown in Fig. 3. (C) Quantitative measurement of expression level changes in the *Peg3* and *Gnas* domains. The initial observations drawn from a fixed number of RT-PCR analyses shown in panel B were analyzed further using quantitative RT-PCR techniques. The upper diagram shows the genomic layout of the *Peg3* domain with the clustered YY1 binding site indicated by ovals. The lower diagram is for the *Gnas* domain. Each gene was analyzed similarly by RT-PCR using four different cells: NT, EV, 6-2, and 6-4. The expression level of each gene was first normalized with three different control genes (*β-actin, GAPDH, 28S*) and later compared with the normalized level of the NT sample. The fold differences compared to the NT sample were presented for each gene. These qRT-PCR results were derived from three independent trials ($n=3$), starting from RNA isolation to qRT-PCR. (D) Quantitative measurement of expression level changes in other genes. The initial observations (in panel B) were analyzed further using qRT-PCR for *GR, Sp1, Snrpn, Ube3a, Tsix*, and *Xist*. Student's *t* test was performed to measure the statistical significance of all the observations drawn from the above results. In most cases, the *p* values were much smaller than 0.05, meeting statistical significance. However, some data points have *p* values greater than 0.05, such as the data set for *Tsix* and the 6-4 data set for *Xist*, and thus the observations regarding these loci need to be further investigated.

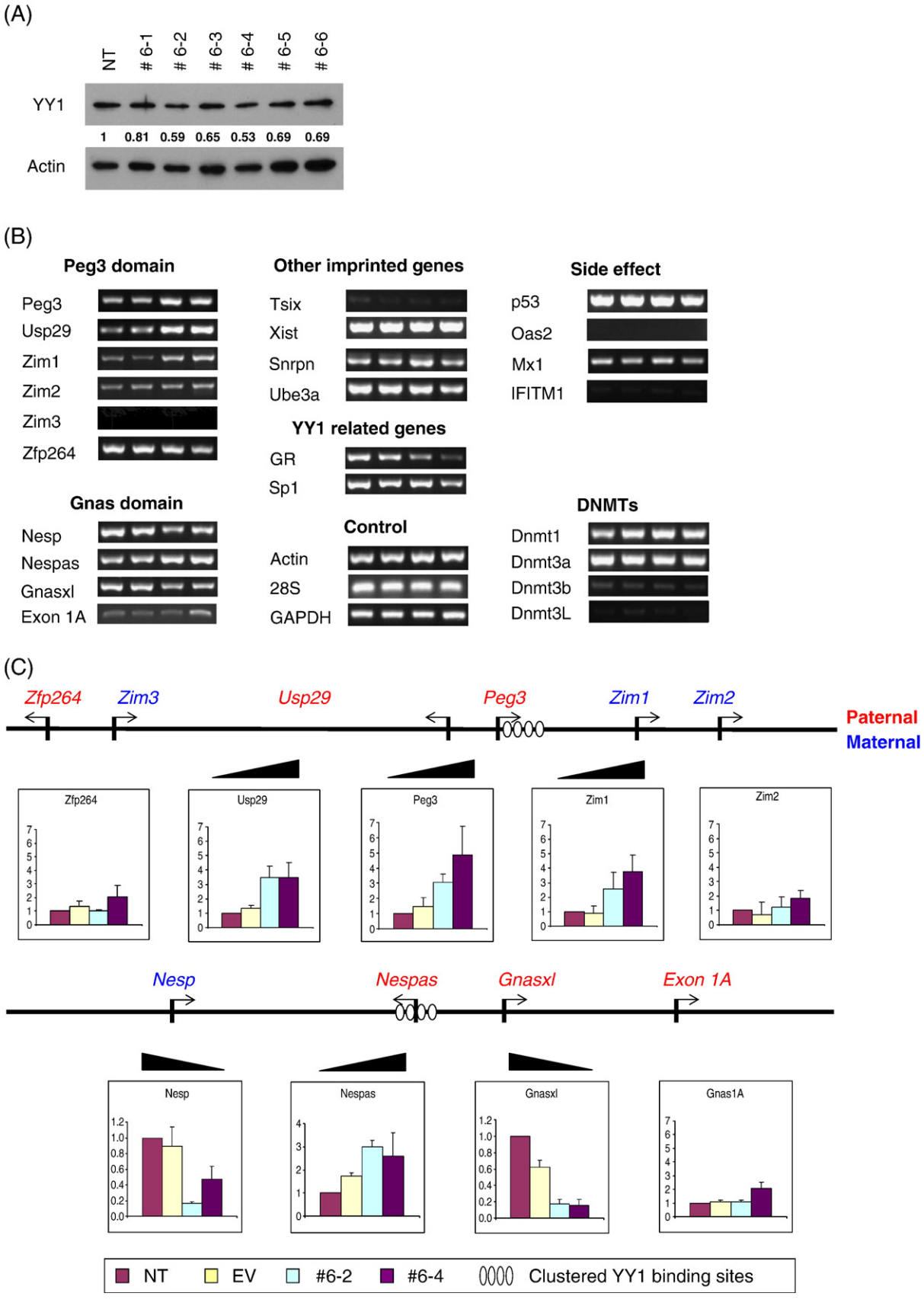
(A)
NT
6-1
6-2
6-3
6-4
6-5
6-6
YY1
1 0.81 0.59 0.65 0.53 0.69 0.69
Actin
(B)
Peg3 domain
Peg3
Usp29
Zim1
Zim2
Zim3
Zfp264
Gnas domain
Nesp
Nespas
Gnasxl
Exon 1A
Other imprinted genes
Tsix
Xist
Snrpn
Ube3a
YY1 related genes
GR
Sp1
Control
Actin
28S
GAPDH
Side effect
p53
Oas2
Mx1
IFITM1
DNMTs
Dnmt1
Dnmt3a
Dnmt3b
Dnmt3L
(C)
Zfp264
Zim3
Usp29
Peg3
Zim1
Zim2
Paternal
Maternal
Nesp
Nespas
Gnasxl
Exon 1A
Gnas1A
NT
EV
#6-2
#6-4
Clustered YY1 binding sites

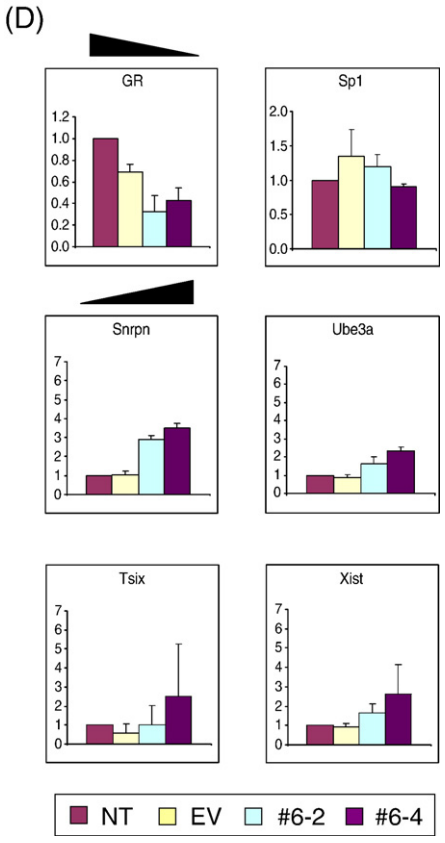

Fig. 2 (*continued*).

2D). Likewise, the expression levels of *Snrpn* were also increased by 3-fold, which agrees well with the independent result derived from the studies of a YY1-deleted mouse [22]. The expression change for GR in YY1 knockdown cells is readily noticeable by both RT-PCR and qRT-PCR, but other YY1-related, nonimprinted genes did not show any major change. Expression levels of many other genes were not affected by YY1 knockdown, including several DNA methyltransferases, CTCF, and macroH2A1 (data not shown). Taken together, long-term YY1 knockdown resulted in changed expression levels for the imprinted genes in the *Peg3* and *Gnas* domains in a somewhat coordinated manner. The observed coordinated response may be an indication that YY1 is involved in the overall regulation of these imprinted domains, possibly through ICRs.

The long-term effects of YY1 knockdown on DNA methylation of imprinted domains

We have also investigated the DNA methylation status of *Peg3, Nespas*, and *Xist* DMRs to analyze potential long-term effects caused by YY1 knockdown. As shown in Fig. 3A, genomic DNAs from four different Neuro2A cells were digested first with *Bam*HI (lane B) and later individually with methylation-insensitive *Msp*I (lane B+M) and methylation-sensitive *Hpa*II (lane B+H). Hybridizations with the two probes covering the promoter and YY1 binding regions of the *Peg3* DMR showed different band patterns between the control cells and the YY1 knockdown cells. In YY1 knockdown cells, the sizes of methylated DNA fragments become smaller (lane B+H), indicating DNA methylation loss in these cells. These initial results were further analyzed by performing bisulfite sequencing (Fig. 3B). We have performed independently another Southern blot using the restriction enzyme *Nar*I, the recognition site of which overlaps with the sequence of YY1 binding sites (*GGCGCC*ATCTT) that are located within the *Peg3* DMR. These results indicated that the CpG sites of the YY1 binding sites also lost DNA methylation in the YY1 knockdown Neuro2A cells (data not shown). These results again confirm the loss of methylation in the *Peg3* DMR. These results are also consistent with the up-regulation of *Peg3* and *Usp29* that we have observed in stable YY1 knockdown experiments (Fig. 2C).

We also performed a similar set of methylation analyses on the DMR of *Nespas*, which is associated with multiple YY1 binding sites (Fig. 3C). In the *Nespas* DMR, one of the knockdown cells, 6-4, showed slightly different patterns compared to those of two control cells, but the significance of this difference is uncertain. Overall, the methylation levels of the *Nespas* DMR did not appear to be affected by YY1 knockdown in Neuro2A cells.

By contrast, the *Xist* locus appears to have reduced levels of DNA methylation in YY1 knockdown cells (Fig. 3D). In the two control cells, two different-sized DNA fragments representing methylated and unmethylated DNA fragments were detected at similar ratios in the *Bam*HI/*Hpa*II double digestion (lane B+H). These two bands are thought to represent the two different X chromosomes of the female-origin Neuro2A cells, active and inactive X chromosomes. In the two knockdown cells, the smaller sized DNA fragment derived from unmethylated DNAs is more dominant, indicating that this particular CpG site has lost its DNA methylation in both YY1 knockdown cell lines. This is consistent with the detection of slight up-regulation of *Xist* in the two YY1 knockdown cells (Fig. 2D). In sum, our DNA methylation analyses indicated that long-term YY1 knockdown results in hypomethylation in the DMRs of *Peg3* and *Xist*, and this change is consistent with the transcriptional up-regulation observed in these two domains.

Discussion

RNAi-based YY1 knockdown experiments demonstrated that lowering YY1 protein levels caused global and somewhat coordinated changes in the expression levels of the genes located in the *Peg3* and *Gnas* domains. The transcriptional up-regulation observed in the *Peg3* domain was also accompanied by changes in the DNA methylation level of the *Peg3* DMR, suggesting a possible role for YY1 in maintaining the proper methylation status of this DMR sequence.

Our recent identification of multiple YY1 binding sites within the ICRs of *Peg3, Nespas*, and *Xist/Tsix* suggests that YY1 plays a role for the imprinting control of these domains [9]. Given the colocalization of YY1 binding sites in these differentially methylated regions, it is likely that YY1 plays a role in maintaining and/or establishing the allele-specific

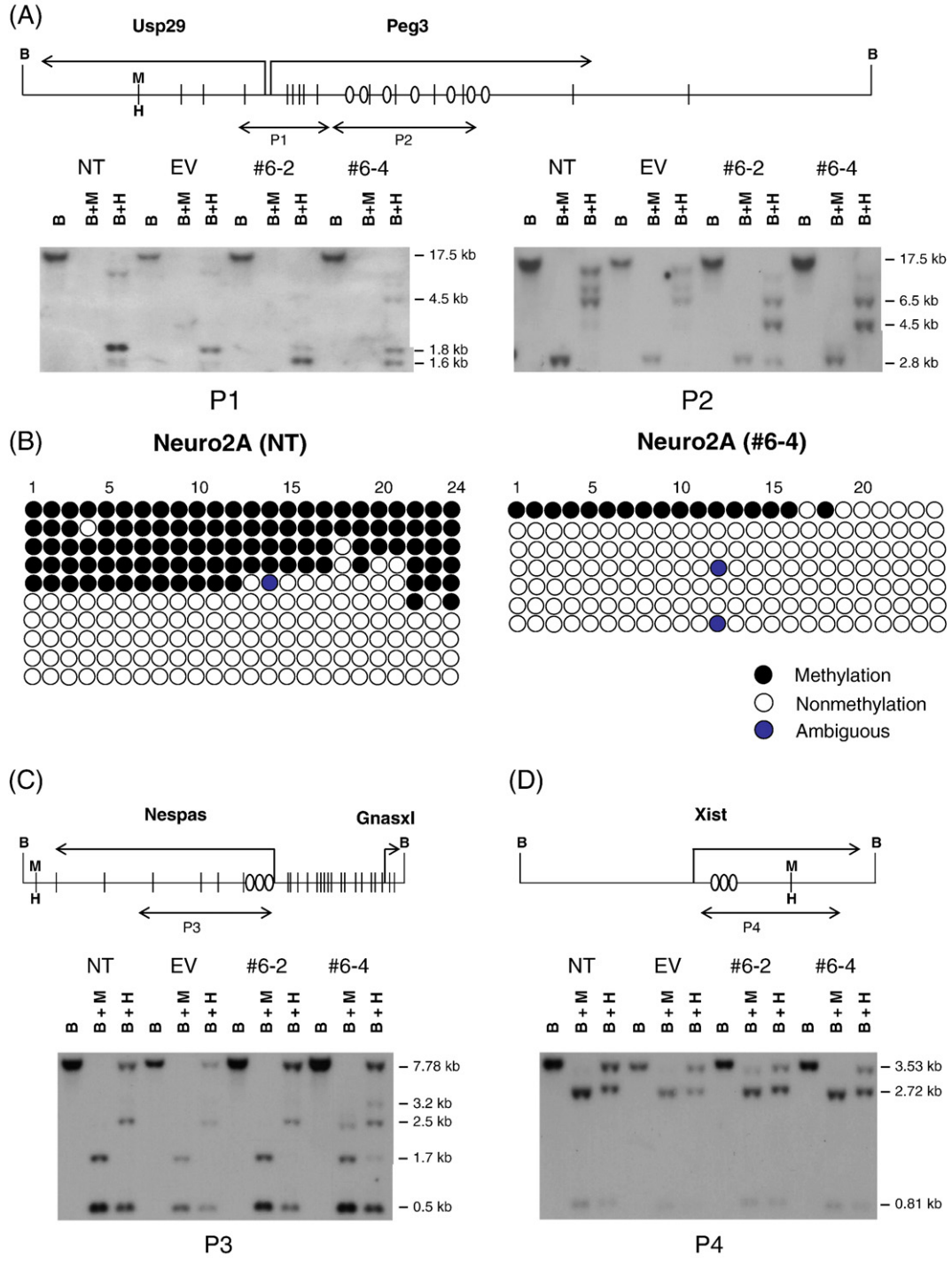

Fig. 3. Long-term effects on the DNA methylation status of the DMRs of (A) *Peg3*, (C) *Nespas*, and (D) *Xist*. The schematic diagram for each DMR is shown at the top, while the results derived from methylation analyses using Southern blot and bisulfite sequencing approaches are shown at the bottom. The schematic diagram shows the relative position of each DMR to *Bam*HI sites (B) and two isoschizomer sites (*Msp*I, methylation-insensitive; *Hpa*II, methylation-sensitive). The diagram also indicates the genomic regions that have been used as probes for Southern blotting, which are marked by double-headed arrows with P1 through P4. The ovals in the diagram represent YY1 binding sites. For the methylation analyses, four different genomic DNAs were isolated from the cells of NT, EV, 6-2, and 6-4. These DNAs were first digested with *Bam*HI (lane B) and later with *Msp*I (lane B+M) or *Hpa*II (lane B+H). (B) Two different DNAs from NT and 6-4 were also analyzed with the bisulfite sequencing method for the methylation analysis of the promoter region of *Peg3*. Each row represents one individual DNA strand derived from this bisulfite conversion reaction, while the 24 circles in each row represent individual CpG sites located within this 430-bp promoter region. Ten different clones were successfully sequenced for the NT sample and 7 clones for the 6-4 sample.

methylation of these regions. Consistently, our data showed that stable knockdown of YY1 resulted in hypomethylation in the DMRs of *Peg3* and *Xist* (Fig. 3). Similar observations have been made in the studies of CTCF binding sites in the *H19* ICR [10,11]. In this case, both ablation of CTCF binding sites within the *H19* ICR and CTCF knockdown in mice resulted in

hypermethylation of the *H19* ICR, suggesting that CTCF may function as a protector for the unmethylated, maternal allele of the *H19* ICR. This is somewhat opposite to the hypomethylation observed in YY1 knockdown stable cells in our experiments (Fig. 3). In the case of the *Peg3* DMR, YY1 may be required for maintaining the methylated status of the inactive maternal allele. One likely scenario would be that YY1 recruits histone-modifying enzymes, such as HDACs, which are, in turn, required for DNA methylation (reviewed in [23]). This is plausible given the numerous interaction partners of YY1 that are involved in epigenetic modifications (reviewed in [13,14]).

In the YY1 knockdown cells, the *Peg3* and *Gnas* domains showed somewhat global and coordinated responses against lowering the YY1 protein levels (Fig. 2C). In both domains, YY1 knockdown affected not a single gene but several genes in each domain. In the *Peg3* domain, although the YY1 binding sites are located right next to the bidirectional promoter of *Peg3* and *Usp29*, the impact of YY1 knockdown was also observed in *Zim2* (transient experiments, Fig. 1) and *Zim1* (stable experiments, Fig. 2). The transcription of all the affected genes in this domain was similarly up-regulated, and this up-regulation was also accompanied with hypomethylation in the *Peg3* DMR (Fig. 3A). In the *Gnas* domain, multiple YY1 binding sites are located in the first intron of *Nespas*, but expression changes were detected in three genes, *Nespas, Nesp*, and *Gnasxl* (Fig. 2C). In particular, the up- and down-regulation of *Nespas* and *Nesp*, respectively, is an expected outcome based on the antisense/sense relationship of the two genes, but only if YY1 is involved directly in the regulation of these two genes. The observed expression changes of the *Nespas/Nesp* pair, therefore, confirm that YY1 is indeed functionally involved in the regulation of the two genes. According to the results derived from mutant mice lacking the *Nespas* DMR, which coincides exactly with the multiple YY1 binding region [24], deletion of this DMR affected the transcription and imprinting of all the genes in this domain. In this case, the absence of *Nespas* expression in the mutant mice resulted in the up-regulation of *Nesp*. This situation appears to be opposite to that represented in YY1 knockdown cells, in which *Nespas* is up-regulated and *Nesp* is down-regulated. Nevertheless, the observed responses in both experiments provide a consistent outcome, a coordinated response between *Nespas* and *Nesp*. Along with the overall up-regulation observed from the *Peg3* domain, this coordinated response supports the idea that YY1 indeed plays a major role in the regulation of these two imprinted domains.

Materials and methods

YY1 knockdown using RNA interference techniques

The sequences of the siRNA constructs used for this study are as follows: YY1 siRNA, sense strand, 5′-GATCCCCGAGAGAACTCACCTCCTGATTCAAGAGATCAGGAGGTGAGTTCTCTCTTTTTGGAAA-3′; YY1 siRNA, antisense strand, 5′-AGCTTTTCCAAAAAGAGAGAACTCACCTCCTGATCTCTTGAATCAGGAGGTGAGTTCTCTCGGG-3′; Scramble siRNA, sense strand, 5′-GATCCCCAGGAGAAATAGGGGGACACTTCAAGAGAGTGTCCCCCTATTTCTCCTTTTTTGGAAA-3′; Scramble siRNA, antisense strand, 5′-AGCTTTTCCAAAAAAGGAGAAATAGGGGGACACTCTCTTGAAGTGTCCCCCTATTTCTCCTGGG-3′. Duplex oligonucleotides were subcloned into the *Bgl*II and *Hin*dIII sites of pSUPER vector (OligoEngine). To make the stable YY1 knockdown cell lines, we first generated one inverted DNA fragment using a DNA fragment derived from the transcribed region of mouse YY1 (GenBank Accession No. NM_009537, position 1222–1607), and later this inverted fragment was subcloned into the 3′-UTR of the pcDNA3.1/His/lacZ vector (Invitrogen). These RNAi vectors were amplified in the *Escherichia coli* Sure 2 strain (Stratagene), which allows the accurate replication of inverted repeat-containing DNAs. These constructs were purified using the HiSpeed plasmid midikit (Qiagen) and transfected into cells using the GeneJuice transfection reagent according to the manufacturer's protocol (Novagen). For stable transfection experiments, transfected cells were selected by adding G418 (500 μg/ml; Calbiochem) to the culture medium.

Western blot

For our Western blot analysis, the cells were lysed 48 h after transfection using lysis buffer (0.25 M Tris–HCl, pH 7.8, plus 0.1% NP-40) for 30 min at 4°C and cellular debris was removed by centrifugation for 10 min. Protein concentrations were determined by the Bradford assay kit (Pierce). Thirty micrograms of lysate was separated on 10% SDS–PAGE gels and transferred to the PVDF membrane (Hybond-P; Amersham) using a Mini Trans-Blot transfer cell (Bio-Rad). Membranes were blocked for 1 h in Tris-buffered saline containing 5% skim milk and 0.05% Tween 100 and incubated at 4°C overnight with anti-YY1 (sc-1703), anti-p53 (sc-6243), or anti-β-actin (sc-1615) antibodies (Santa Cruz Biotechnology). These blots were incubated for an additional 1 h with the secondary antibody linked to horseradish peroxidase (Sigma). The blots were developed using a Western blot detection system according to the manufacturer's protocol (Intron Biotech).

RT-PCR and quantitative PCR

Total RNAs were first purified from transfected cells using Trizol as described by the manufacturer (Invitrogen); second, first-strand cDNA was reverse transcribed using the SuperScript First-Strand Synthesis System (Invitrogen); and finally PCR amplifications were performed with a series of specific primer pairs using the Maxime PCR premix kit (Intron Biotech). Also, quantitative real-time PCR was performed with iQ SYBR Green Supermix (Bio-Rad) using the icycler iQ multicolor real-time detection system (Bio-Rad). All qPCRs were carried out for 40 cycles under standard PCR conditions. We analyzed the results of quantitative real-time PCR based on the threshold cycle value. A ΔC_t was first calculated by subtracting the averaged C_t value of three internal controls from the averaged C_t value of a target gene, and later the $\Delta\Delta C_t$ value was calculated by subtracting the ΔC_t value for the targeted gene of a YY1 knockdown sample from the ΔC_t value for that of the control. Fold differences were determined by raising 2 to the $\Delta\Delta C_t$ power [25]. The primer sequences and PCR conditions are available upon request.

Southern blot and bisulfite sequencing

Genomic DNAs were purified using DNAzol (Invitrogen), and 5 μg of each genomic DNA was first digested with *Bam*HI and later with either *Msp*I or *Hpa*II. These double-digested DNAs were separated on a 0.8% agarose gel and transferred by capillary blotting onto Hybond nylon membranes (Amersham). Membranes were hybridized with the ^{32}P-labeled probes as indicated in the figures and analyzed by autoradiography. The probes used for this study are as follows: a 1.3-kb fragment corresponding to the *Peg3* promoter, a 2.3-kb fragment for the *Peg3* YY1 binding region, a 1.95-kb fragment for the *Nespas* YY1 binding region, and a 1.88-kb fragment of the *Xist* YY1 binding region. The methylation status of the promoter region of mouse *Peg3* (GenBank Accession No. AC020961; 106803–107240) was also analyzed using the bisulfite sequencing method [26]. The DNAs isolated from NT and 6-4 were first digested with *Bam*HI, purified with phenol/chloroform extraction, and precipitated with ethanol. For the bisulfite conversion reaction, these DNAs were treated with the EZ DNA methylation kit (Zymo Research). The resultant single-stranded DNAs were used as templates for the PCR

using specific primers that were designed for the C-to-T converted DNAs. The sequences for these primers are as follows: *Peg3* Promoter F, 5′-AGAGGGTGTTGTAGAGTAGTTAGGTG-3′, and *Peg3* Promoter R, 5′-CATCCCTTCACACCCACATCCCATCC-3′. The PCR products were subcloned into the TOPO TA cloning vector (Invitrogen) for sequencing.

Acknowledgments

We thank Dr. Prescott Deininger for critically reading the manuscript. This research was supported by National Institutes of Health R01 GM66225, National Science Foundation EPS-0346411, and the State of Louisiana Board of Regents Support Fund (J.K).

References

[1] M.S. Bartolomei, S.M. Tilghman, Genomic imprinting in mammals, Annu. Rev. Genet. 31 (1997) 493–525.
[2] C.I. Brannan, M.S. Bartolomei, Mechanisms of genomic imprinting, Curr. Opin. Genet. Dev. 9 (1999) 164–170.
[3] L. Spahn, D.P. Barlow, An ICE pattern crystallizes, Nat. Genet. 35 (2003) 11–12.
[4] M. Constancia, B. Pickard, G. Kelsey, W. Reik, Imprinting mechanisms, Genome Res. 8 (1998) 881–900.
[5] W. Reik, J. Walter, Imprinting mechanisms in mammals, Curr. Opin. Genet. Dev. 8 (1998) 154–164.
[6] A.C. Bell, G. Felsenfeld, Methylation of a CTCF-dependent boundary controls imprinted expression of the *Igf2* gene, Nature 405 (2000) 482–485.
[7] A.T. Hark, C.J. Schoenherr, D.J. Katz, R.S. Ingram, J.M. Levorse, S.M. Tilghman, CTCF mediates methylation-sensitive enhancer-blocking activity at the H19/Igf2 locus, Nature 405 (2000) 486–489.
[8] J. Kim, A. Kollhoff, A. Bergmann, L. Stubbs, Methylation-sensitive binding of transcription factor YY1 to an insulator sequence within the paternally expressed imprinted gene, Peg3, Hum. Mol. Genet. 12 (2003) 233–245.
[9] J.D. Kim, et al., Identification of clustered YY1 binding sites in imprinting control regions, Genome Res. 16 (2006) 901–911.
[10] C.J. Schoenherr, J.M. Levorse, S.M. Tilghman, CTCF maintains differential methylation at the Igf2/H19 locus, Nat. Genet. 33 (2003) 66–69.
[11] A.M. Fedoriw, P. Stein, P. Svoboda, R.M. Schultz, M.S. Bartolomei, Transgenic RNAi reveals essential function for CTCF in H19 gene imprinting, Science 303 (2004) 238–240.
[12] Y. Shi, J.S. Lee, K.M. Galvin, Everything you ever wanted to know about Yin Yang 1, Biochim. Biophys. Acta 1334 (1997) F49–F66.
[13] M.J. Thomas, E. Seto, Unlocking the mechanisms of transcription factor YY1: are chromatin modifying enzymes the key? Gene 236 (1999) 197–208.
[14] S. Gordon, G. Akoryan, H. Garban, B. Bonavida, Transcription factor YY1: structure, function, and therapeutic implications in cancer biology, Oncogene 25 (2006) 1125–1142.
[15] J.L. Brown, D. Mucci, M. Whiteley, M.L. Dirksen, J.A. Kassis, The Drosophila Polycomb group gene pleiohomeotic encodes a DNA binding protein with homology to the transcription factor YY1, Mol. Cell 1 (1998) 1057–1064.
[16] D.P.E. Satijn, K.M. Hamer, J.D. Blaawen, A.P. Otte, The polycomb group protein EED interacts with YY1, and both proteins induce neural tissue in Xenopus embryos, Mol. Cell. Biol. 21 (2001) 1360–1369.
[17] G. Caretti, M. Di Padova, B. Micales, G.E. Lyons, V. Sartorelli, The Polycomb Ezh2 methyltransferase regulates muscle gene expression and skeletal muscle differentiation, Genes Dev. 18 (2004) 2627–2638.
[18] K.S. Khabar, et al., Effect of deficiency of the double-stranded RNA-dependent protein kinase, PKR, on antiviral resistance in the presence or absence of ribonuclease L: HSV-1 replication is particularly sensitive to deficiency of the major IFN-mediated enzymes, J. Interferon Cytokine Res. 20 (2000) 653–659.
[19] C.A. Sledz, M. Holko, M.J. de Veer, R.H. Silverman, B.R.G. Williams, Activation of the interferon system by short-interfering RNAs, Nat. Cell Biol. 5 (2003) 834–839.
[20] F. Relainx, et al., Pw1, a novel zinc finger gene implicated in the myogenic and neuronal lineages, Dev. Biol. 177 (1996) 383–396.
[21] S. Rodriguez-Jato, R.D. Nicholls, D.J. Driscoll, T.P. Yang, Characterization of cis- and trans-acting elements in the imprinted human SNURF–SNRPN locus, Nucleic Acids Res. 33 (2005) 4740–4753.
[22] E.B. Affar, F. Gay, Y. Shi, H. Liu, M. Huarte, S. Wu, T. Collins, E. Li, Y. Shi, Essential dosage-dependent functions of the transcription factor yin yang 1 in late embryonic development and cell cycle progression, Mol. Cell. Biol. 26 (2006) 3565–3581.
[23] R. Jaenisch, A. Bird, Epigenetic regulation of gene expression: how the genome integrates intrinsic and environmental signals, Nat. Genet. Suppl. (2003) 245–254.
[24] C.M. Williamson, et al., Identification of an imprinting control region affecting the expression of all transcripts in the Gnas cluster, Nat. Genet. 38 (2006) 350–355.
[25] J. Winer, C.K. Jung, I. Shackel, P.M. Williams, Development and validation of real-time quantitative reverse transcriptase-polymerase chain reaction for monitoring gene expression in cardiac myocytes in vitro, Anal. Biochem. 270 (1999) 41–49.
[26] M. Frommer, et al., A genomic sequencing protocol that yields a positive display of 5′-methylcytosine residues in individual DNA strands, Proc. Natl. Acad. Sci. USA 89 (1992) 1827–1831.